Lifetimes of the $3p^5 4s\ ^3P_1$, $^1P_1$ and $3p^5 3d\ ^3P_1$ levels in K II

M. Henderson, L. J. Curtis, R. Matulioniene, and D. G. Ellis
Department of Physics and Astronomy, University of Toledo, Toledo, Ohio 43606

Yuelin Li
Institut für Optik und Quantenelektronik, Friedrich-Schiller-Universität, D-07743 Jena, Germany

(Received 29 October 1996; revised manuscript received 18 December 1996)

Oscillator strengths for the three lowest ground-state transitions $3p^6\ ^1S_0$-$3p^5 4s\ ^3P_1$, $3p^6\ ^1S_0$-$3p^5 4s\ ^1P_1$, and $3p^6\ ^1S_0$-$3p^5 3d\ ^3P_1$ in argonlike K II are reported. The values were determined by lifetime measurements made using foil excitation of a fast ion beam, which yielded values $\tau(4s\ ^3P_1)=8.4\pm1.6$ ns, $\tau(3d\ ^3P_1)=2.4\pm0.4$ ns, and $\tau(4s\ ^1P_1)=0.43\pm0.04$ ns. Application of these results to the development of extreme ultraviolet lasers is discussed. [S1050-2947(97)05304-3]

PACS number(s): 32.70.Cs

I. INTRODUCTION

Lifetime studies of inert-gaslike transitions of the form np^6-$np^5(n+1)s$ are interesting for a number of reasons. They provide a rare case in which $\Delta n=1$ transitions are unbranched, and thus permit oscillator strengths to be determined directly from lifetime measurements. The nominal $^1S_0$-$^1P_1$ resonance and $^1S_0$-$^3P_1$ intercombination transitions are heavily spin hybridized, and provide competing channels under the conditions of intermediate coupling that are characteristic of these systems. Moreover, the intershell nature of the $\Delta n=1$ transitions causes them to have substantially shorter wavelengths (and hence shorter lifetimes) than would the corresponding $\Delta n=0$ transitions in, e.g., an ns^2-$nsnp$ alkaline-earthlike system.

A prominent application of knowledge about the lifetimes of $np^5(n+1)s$ levels concerns singly ionized alkali-metal atoms, which is closely related to extreme ultraviolet (XUV) laser development using the inner-shell photoionization scheme proposed by Duguay and Retzenpis [1]. The scheme utilizes the characteristic nature of the $n=2$ (and $n=3$) cases for which the probability of ejecting a $2p$ ($3p$) electron from a Na (K) atom is about 100 times larger than that of ejecting the $3s$ ($4s$) electron by photoionization with photon energies larger than the $2p$ ($3p$) threshold. This leads to population inversion between the $2p^5 3s$ and $2p^6$ ($3p^5 4s$ and $3p^6$) states and lasing at 372 (601) Å. Such a scheme has a higher quantum efficiency than those pumped by electron collisional excitation or recombination due to the lower ionization state involved. Lasing in K II on the $3p^6$-$3p^5 4s$ transition is more advantageous due to the larger cross section for stimulated emission resulting from the longer lasing wavelength, as well as the larger photoionization cross section. Though earlier experimental efforts failed to show lasing in both materials [2,3], the recent development of high power ultrashort pulse laser systems has brought a renewed possibility to demonstrate these lasers [4]. In this case, knowledge about the lifetime of the $np^5(n+1)s$ levels is obviously very important for theoretical calculation of the population dynamics and estimation of the gain, as well as the experimental measurement of the laser.

Thus we report here oscillator strength measurements for transitions that have not previously been studied experimentally, both to elucidate the conditions of heavy configuration interaction that are present, and to provide data that are needed for a related area of current research.

II. THEORY

The theoretical specification of the $3p^5 4s$ lifetimes in K II involves special problems not encountered either for other members of the Ar isoelectronic sequence, or for the $2p^5 3s$ lifetimes in the homologous Na II ion in the Ne sequence. This is illustrated in Fig. 1, which isoelectronically plots measured $J=1$ energy levels of the $3p^5 4s$ and $3p^5 3d$ configurations, scaled to the corresponding ionization energy of the $3p^6$ ground state, for Ar I [5], K II [6,7], Ca III [8], Sc IV [9], Ti V [10], and V VI [11]. The plunging of the $3p^5 3d$ levels, caused by the collapse of the $3d$ orbital [12], leads to strong configuration interaction (CI) for K II ($Z=19$) where $3p^5 3d\ ^3P_1$ is interposed between the $3p^5 4s\ ^3P_1$ and $^1P_1$, and for Sc IV ($Z=21$) where the $3p^5 3d\ ^1P_1$ lies just above the $3p^5 4s\ ^1P_1$. It should be noted

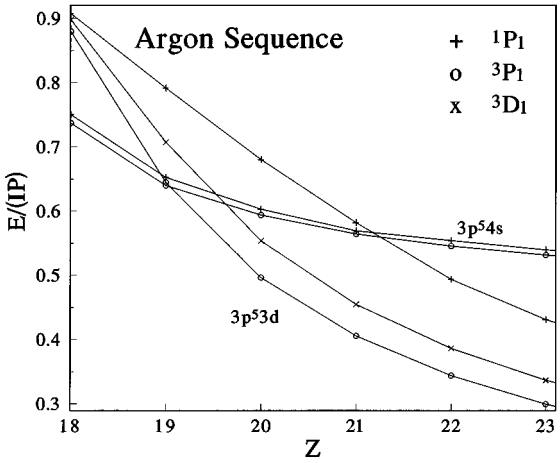

FIG. 1. Isoelectronic plot of the $J=1$ energy levels of the $3p^5 4s$ and $3p^5 3d$ configurations, divided by the ground-state ionization potential.

TABLE I. Theoretical energies and eigenvectors.

	$4s\ ^3P_1$		$3d\ ^3P_1$		$4s\ ^1P_1$	
	HFR/ADJ	MCDF/OL3	HFR/ADJ	MCDF/OL3	HFR/ADJ	MCDF/OL3
E (kK)	163.223	152.396	164.533	155.048	166.457	156.129
$\langle 4s\ ^3P\|\psi\rangle$	0.76	0.84	−0.51	−0.20	−0.41	−0.50
$\langle 3d\ ^3P\|\psi\rangle$	0.59	0.45	0.79	0.77	0.12	0.45
$\langle 4s\ ^1P\|\psi\rangle$	0.26	0.29	−0.34	−0.60	0.90	0.74

that LS coupling labels are only nominal in the presence of such strong CI, and labeling conventions must be carefully defined in a situation in which the energy levels undergo an avoided crossing whereas the eigenvectors undergo a crossing [13].

The homologous $2p^6$-$2p^5 3s$ transitions in the Ne sequence are not affected by plunging levels, and in that system it has been shown [14–16] that the energy levels, transition probabilities, and the magnetic g factors all can be formulated in terms of a set of single configuration intermediate coupling amplitudes. A similar formulation has been made for Ar I [14,17], Ca III [18], and argonlike ions with $Z \geqslant 22$ [14], but for K II and Sc IV it has been shown [18] that CI mixing with $3p^5 3d$ must be included.

Since there are no recent calculations of these transitions, and the energy-level data suggest the possibility of strong mixing, we have done two kinds of calculations for comparison with our experimental results. First we used the Cowan programs RCN-RCG in the Hartree-Fock relativistic (HFR) mode [19]. The eigenvectors and lifetimes labeled HFR/ADJ in Table I are from a calculation using configurations $3p^6$, $3p^5 4s$, $3p^5 5s$, $3p^5 3d$, and $3p^5 4d$, with empirical adjustments (ADJ) of Slater parameters to reproduce the observed energies of the seven $4s\ ^3P$, $4s\ ^1P$, and $3d\ ^3P$ levels. Larger RCN-RCG calculations without empirical adjustments did not give the correct energy ordering of the lowest three $J^P = 1^-$ levels. The calculation with empirical adjustments also gave good agreement with the observed g factors, which provide a clear distinction between the two lowest (nominally triplet) levels and the third (nominally singlet) level.

We also used the multiconfiguration Dirac-Fock (MCDF) program GRASP [20] to get a Dirac-based relativistic treatment of the complicated interactions in this case. We found that the correct energy ordering of the three lowest $J^P = 1^-$ levels could be obtained by an extended optimal level (OL) calculation including only the $3p^6$, $3p^5 4s$, and $3p^5 3d$ configurations (six relativistic configurations), and optimizing on the three levels of interest. The eigenvectors predicted by this calculation are labeled MCDF/OL3 in Table I. Here also we found that larger calculations did not lead easily to a converged or obviously improved solution. The lifetimes obtained by these methods are given in Table II.

These two calculations, although far from a theoretical solution to the problem, provide convincing evidence that all three levels are strongly mixed, and that the two lowest are most reasonably identified as the triplets but with lifetimes less than 10 ns. An *ab initio* calculation of the level energies, g factors, and transition probabilities in this $4s$-$3d$ complex would be a significant test of theory because of the importance of both relativity and correlation.

III. EXPERIMENT

This experiment utilized the University of Toledo Heavy Ion Accelerator, and detailed descriptions of this facility are provided in reports of earlier studies [21,22] and instrumentation reviews [23,24]. The beam-foil excitation method permits time-resolved studies of a low-density source in an environment that is free of electric and magnetic fields, interparticle collisions, and radiation trapping, and numerous

TABLE II. Lifetimes and oscillator strengths.

Level	λ (Å)[a]	τ (ns)			f
		Expt.[b]	Theory[b]	Other theory	Expt.[b]
$3p^5 4s\ ^3P_1$	612.6	8.4±1.6	5.6,[c] 5.1,[d] 7.7[e]	2.9,[f] 3.3[g]	0.020±0.004
$3p^5 3d\ ^3P_1$	607.9	2.4±0.4	2.9,[c] 1.1,[d] 1.5[e]	104,[f] 3800,[g] 800,[h] 775[i]	0.069±0.012
$3p^5 4s\ ^1P_1$	600.7	0.43±0.04	0.42,[c] 0.76,[d] 1.05[e]	0.45,[f] 0.46[g]	0.38±0.04
$3p^5 3d\ ^3D_1$	554.2		94[c]	91,[f] 68,[g] 84,[h] 65[i]	
$3p^5 3d\ ^1P_1$	495.1		0.015[c]	0.13,[f] 0.056,[g] 0.014,[h] 0.07[i]	

[a]Refs. [6] and [18].
[b]This work.
[c]HFR/ADJ.
[d]MCDF (Coulomb gauge).
[e]MCDF (Babushkin gauge).
[f]Loginov and Gruzdev, Ref. [30].
[g]Lin *et al.*, Ref. [31].
[h]Cowan, Ref. [12].
[i]Cowan, Ref. [29].

extensive reviews of its application are available [25,26]. Ions of K^+ were produced in the ion source, accelerated through 20 kV, and magnetically analyzed. After momentum and mass-to-charge ratio selection, the ions were postaccelerated to final energies of 220 keV. The ions then entered an electrostatic switchyard and were steered into the experimental station and collimated before passage through a thin (2.1–2.5 $\mu g/cm^2$) carbon foil. The decay curves were measured by recording the intensity of the spectral lines as a function of distance downstream from the foil. The experiment was controlled by a CAMAC based data acquisition system with a Pentium 120 MHz computer interfacing it via the Linux operating system.

Using the Danfysik Model 911A ion source, ions were obtained from potassium iodide. No carrier gas was necessary, and ions were produced as soon as the source filament current reached 20 A. To control the discharge, the anode power was set at nearly zero (e.g., at 0.1 A and 10 V). Under these conditions the singly charged beam dominated the ion source production.

Energy levels, spectroscopic classifications, and wavelength lists are available for K I–IV [6,27], which are the ionization stages accessible at the beam energies used. The K II emission lines were analyzed with an Acton 1-m normal incidence vacuum ultraviolet monochromator, with two sets of concave gratings and detectors: a 2400-l/mm grating blazed at 800 Å coupled with a channeltron detector for the three transitions of interest; and a 600-l/mm grating blazed at 3000 Å coupled with a bialkali detector to attempt to scan for the cascade transitions that repopulate them. At these 220-keV beam energies, the observed lines were of K I through K IV [27], and the average foil-in–foil-out charge ratio was between 1.5 and 1.75. Under these conditions, the semiempirical formula of Nikolaev and Dimitriev [28] predicts foil-emergent charge state fractions of 4% for K I, 51% for K II, 43% for K III, and 2% for K IV. The post foil velocity was determined to within 2.5% by taking into account uncertainties in energy calibration, foil thickness, and possible beam divergence. The post-foil velocity was 1.002 mm/ns. The optical system viewed a segment of the beam 1 mm in length, and the decay could be followed for 18 mm downstream with no significant escape of particles from the viewing volume due to beam divergence. With this velocity and geometry, the range of lifetime values accessible to measurement was from a few tenths of a ns to about 20 ns.

IV. RESULTS AND ANALYSIS

A spectral scan in the region 598–614 Å is shown in Fig. 2. Gaussian fits to the line profiles are indicated, and yield an instrumental full width at half maximum (FWHM) of 0.52 Å(or a Gaussian 1/e full width of 0.62 Å). This is consistent with the Doppler width of this moving light source due to the finite acceptance angle of the optical detection system. As can be seen, the 600.7-, 607.9-, and 612.6-Å lines are all strong, well separated, free of blends, and have only a small (30 counts/s) beam-associated background between the lines.

This fitting procedure was carried out using the nonlinear least-squares multiexponential fitting program DISCRETE [34]. The 600.7-Å decay curve was easily fitted by two exponentials differing by a factor of 20 in lifetime and of 8 in initial intensity. The 612.6-Å decay curve (an example of which is shown in Fig. 3) was a pure single exponential with no cascades resolvable by exponential curve fitting techniques (see discussion of additional tests of cascading below). The 607.9-Å decay curve was also fitted to two exponentials, but they were closer in lifetime and relative intensity than the 600.7-Å case. A search for likely cascade feeding transitions was made in an attempt to make a correlated decay curve (ANDC) [32,33] analysis, but the corresponding lines were too weak to be used for this purpose. The uncertainty limits set on the 607.9 Å were increased to account for the uncertainties introduced by the possible cascading.

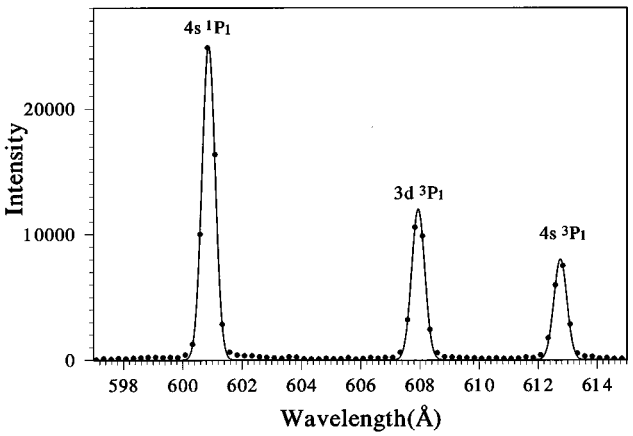

FIG. 2. Spectral scan in the region of the measurements. The curves indicate Gaussian fits to the line profiles, which yield a FWHM of 0.52 Å.

The most likely source of cascade repopulation of the $3p^5 4s$ levels is from the $3p^5 4p$ levels. The lifetimes of these levels have been measured by a number of authors [35–39]. The most recent of these measurements [35] were made by cascade-free laser excitation techniques and yield values of 6.89–7.7 ns, and earlier beam-foil measurements ranged from 7.5 to 10 ns. Although the former may be a better estimate of the $3p^5 4p$ lifetimes, the latter may be a better

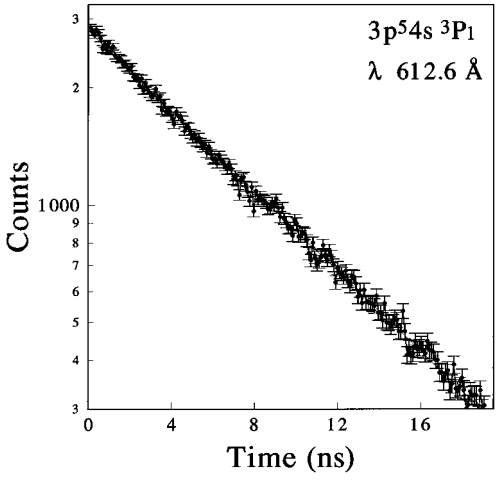

FIG. 3. Typical decay curve of the nominally $3p^5 4s\ ^3P_1$ level measured in the transition at 612.6 Å. The initial point $t=0$ is immediately downstream from the foil.

measure of the indirect and direct cascading that repopulates the $3p^5 4s$ levels. Since we obtained values slightly larger than 8 ns for our measurements of both the single exponential fit to the 612.6-Å line and the longer component in the two exponential fit to the 600.7 Å, possible effects of cascade repopulation of the 612.6-Å line were also considered. Since it is difficult to detect the presence of two nearly equal lifetimes by multiexponential curve fitting methods, we used an alternative fitting approach to estimate the uncertainties that such a possibility could introduce.

For cases in which a primary level of lifetime τ is repopulated by a cascade of similar lifetime $\tau+\Delta\tau$, the time dependence of the emitted intensity $I(t)$ can be expanded [40]:

$$I(t)=I(0)e^{-t/\tau}\left[1+\frac{N_2(0)A_{21}}{N_1(0)}\left(t-\frac{\Delta\tau}{2\tau^2}t^2\right)+\cdots\right], \quad (1)$$

where the $N_1(0)$ and $N_2(0)$ are the initial populations of primary and cascade levels and A_{21} is the transition probability between them. A least-squares adjustment of Eq. (1) to our data for the 612.6-Å line yielded values $\tau=6.4$ ns and $\tau+\Delta\tau=9.6$ ns. Although this fit requires more parameters and was not superior to that obtained using a single exponential, it nonetheless provides an estimate of the range of similar lifetimes that could combine to mimic the single exponential behavior observed in Fig. 3. Thus, although there is no evidence that the cascade repopulation of the 612.6-Å decay curve is strong, and the value obtained directly from curve fitting (8.35 ± 0.04 ns) may well be an accurate measurement of the $4s\ ^3P_1$ lifetime, based on the analysis using Eq. (1) we have increased the uncertainty bounds on the measurement to ±1.6 ns.

The lifetime and oscillator strengths results are summarized in Table II, together with our present and the earlier calculations. Our results suggest that the earlier calculations did not sufficiently account for the strong interactions between these levels, particularly so in the case of the $3p^5 3d\ ^3P_1$. (However, it should be noted that the column labeled ''Other Theory'' is the reciprocal of the transition probability for the $E1$ channel only, and provides only an upper limit to the lifetime for theoretical calculations that yield a small value for that quantity.)

We conclude that our measurements are accurate to the indicated precision, which should be sufficient for use in applications such as population dynamics in XUV lasers.

ACKNOWLEDGMENTS

The work was supported by the U.S. Department of Energy, Office of Basic Energy Sciences, Division of Chemical Sciences, under Grant No. DE-FG02-94ER14461. Y.L. acknowledges support from the State of Thuringia (Germany) under Grant No. B501-95010.

[1] M.A. Duguay and P.M. Rentzepis, Appl. Phys. Lett. **10**, 350 (1967).
[2] E.J. McGuire and M.A. Duguay, Appl. Opt. **16**, 83 (1977).
[3] C.P.J. Barty, G.Y. Yin, J.E. Field, S.J. Benerofe, J.F. Young, and S.E. Harris, in *X-Ray Lasers 1990*, edited by G.J. Tallents (Institute of Physics, Bristol England, 1991), p. 21.
[4] Y. Li, H. Schillinger, Ch. Ziener, and R. Sauerbrey, Opt. Commun. (to be published).
[5] L. Minnhagen, J. Opt. Soc. Am. **63**, 1185 (1973).
[6] C. Corliss and J. Sugar, J. Phys. Chem. Rev. Data **8**, 1109 (1979).
[7] L. Minnhagen (unpublished).
[8] J. Sugar and C. Corliss, J. Phys. Chem. Ref. Data **8**, 865 (1979).
[9] J. Sugar and C. Corliss, J. Phys. Chem. Ref. Data **9**, 473 (1980).
[10] C. Corliss and J. Sugar, J. Phys. Chem. Ref. Data **8**, 1 (1979).
[11] J. Sugar and C. Corliss, J. Phys. Chem. Ref. Data **7**, 1191 (1978).
[12] R.D. Cowan, J. Opt. Soc. Am. **58**, 924 (1968).
[13] S.T. Maniak and L.J. Curtis, Phys. Rev. A **42**, 1821 (1990).
[14] P.W. Murphy, Astrophys. J. **153**, 301 (1968).
[15] L.J. Curtis, Phys. Rev. A **40**, 6958 (1989).
[16] L.J. Curtis, S.T. Maniak, R.W. Ghrist, R.E. Irving, D.G. Ellis, M. Henderson, M.H. Kacher, E. Träbert, J. Granzow, P. Bengtsson, and L. Engström, Phys. Rev. A **51**, 4575 (1995).
[17] N.L.S. Martin, J. Phys. B **17**, 163 (1984).
[18] M. Aymar and M.G. Schweighofer, Physica **67**, 585 (1973).
[19] R.D. Cowan, *The Theory of Atomic Structure and Spectra* (University of California Press, Berkeley, 1981).
[20] K.G. Dyall, I.P. Grant, C.T. Johnson, F.A. Parpia, and E.P. Plummer, Comput. Phys. Commun. **55**, 425 (1989)
[21] M. Henderson, P. Bengtsson, J. Corcoran, L.J. Curtis, R.E. Irving, and S.T. Maniak, Phys. Scr. **53**, 309 (1996).
[22] D.J. Beideck, L.J. Curtis, R.E. Irving, S.T. Maniak, R. Hellborg, S.G. Johansson, A.A. Joueizadeh, I. Martinson, and T. Brage, Phys. Rev. A. **47**, 884 (1993).
[23] R.R. Haar, D.J. Beideck, L.J. Curtis, T.J. Kvale, A. Sen, R.M. Schectman, and H.W. Stevens, Nucl. Instrum. Methods B **79**, 746 (1993).
[24] R.R. Haar and L.J. Curtis, Nucl. Instrum. Methods B **79**, 782 (1993).
[25] E.H. Pinnington, in *Atomic, Molecular, & Optical Physics Handbook*, edited by G.W.F. Drake (AIP Press, New York, 1996), pp. 213–219 and references cited therein.
[26] L.J. Curtis, in *Beam-Foil Spectroscopy*, edited by S. Bashkin (Springer-Verlag, Berlin, 1976), pp. 63–109.
[27] R.L. Kelly and L.J. Palumbo, U.S. GPO, NRL Report No. 7599, 1973 (unpublished).
[28] V.S. Nikolaev and I.S. Dimitriev, Phys. Lett. A **28**, 277 (1968).
[29] R.D. Cowan, J. Phys. (Paris) Colloq. **31** C4-191 (1970).
[30] A.V. Loginov and P.F. Gruzdev, Opt. Spectrosk. **35**, 994 (1973) [Opt. Spectrosc. (USSR) **35**, 578 (1973)].
[31] D.L. Lin, W. Fielder, Jr., and L. Armstrong, Jr., Phys. Rev. A **16**, 589 (1977).
[32] L. Engström, Nucl. Instrum. Methods **202**, 369 (1982).
[33] L.J. Curtis, H.G. Berry, and J. Bromander, Phys. Lett. A **34**, 169 (1971).

[34] S.W. Provencher, J. Chem. Phys. **64**, 2772 (1976).
[35] A. Arnesen, A. Wännström, R. Hallin, C. Nordling, and O. Vogel, J. Opt. Soc. Am. B **5**, 2204 (1988).
[36] H.G. Berry, J. Bromander, and R. Buchta, Phys. Scr. **1**, 179 (1970).
[37] T. Andersen, J. Désesquelles, K. A. Jessen, and G. Sørensen, J. Opt. Soc. Am. **60**, 1199 (1970).
[38] M.C. Poulizac and J.P. Buchet (unpublished).
[39] C.K. Kumar, G.E. Assousa, L. Brown, and W.K. Ford, Jr., Phys. Rev. A **7**, 112 (1973).
[40] A. Denis, P. Ceyzériat, and M. Dufay, J. Opt. Soc. Am. **60**, 1186 (1970).